J Pharmacol Sci 97, 457 – 460 (2005)

Journal of Pharmacological Sciences

Correspondence

Does Proteosome Inhibition Decrease or Accelerate Toxin-Induced Dopaminergic Neurodegeneration?

Rieko Setsuie[1], Tomohiro Kabuta[1], and Keiji Wada[1,*]

[1]*Department of Degenerative Neurological Diseases, National Institute of Neuroscience, National Center of Neurology and Psychiatry, 4-1-1 Ogawahigashi, Kodaira, Tokyo 187-8502, Japan*

Received February 25, 2005

Abstract. Parkinson's disease (PD) is pathologically characterized by dopaminergic (DA) cell death and the presence of Lewy bodies (LB) in the brain. α-Synuclein (α-syn) and ubiquitin (Ub) are the major components of LB, however, the process of their accumulation and their relationship to DA cell loss has not yet been resolved. Now, in this journal, Inden et al. showed the protective effect of proteasome inhibitors (PSI) on DA cell death in the rat PD model using 6-hydroxyl dopamine (6-OHDA). Co-administration of PSI, lactacystin, or MG-132 significantly prevented the nigral degeneration and apomorphine-induced rotational asymmetry of the model with increased appearance of α-syn- and Ub-positive inclusions in the substantia nigra. This study indicates that in their model, accelerated formation of inclusions via proteasome inhibition protects against DA cell death. Previous literature linked the impairments or inhibitions of the ubiquitin-proteasome system (UPS) and DA cell death. However, this report implies that the relationship between the UPS and the pathogenesis of PD may be more complex than we thought.

Keywords: Parkinson's disease, 6-hydroxyl dopamine, proteasome, dopamine

Parkinson's disease (PD) is a progressive neurodegenerative disorder characterized by the impairment of motor function including bradykinesia, resting tremor, rigidity, gait abnormalities, and postural instability. Pathologically, PD is marked by the selective loss of dopaminergic (DA) neurons in the substantia nigra pars compacta (SNpc) and the presence of intracytoplasmic proteinaceous inclusions known as Lewy bodies (LB). Although the molecular mechanism of DA cell death is not fully understood, both genetic and environmental components are believed to contribute significantly to the neurodegenerative process. Among them, dysfunction of the ubiquitin-proteasome system (UPS), a major route for removal of oxidized, damaged, or misfolded proteins, is one of the factors related to the pathogenesis of PD.

Although the large majority of PD cases seem to occur sporadically, infrequent familial forms of PD could turn out to be highly instructive as regards to the pathogenesis of the sporadic PD. To date, six genes have been linked to familial PD: Parkin (1), DJ-1 (2), PTEN-induced kinase 1 (PINK1) (3), leucine-rich repeat kinase 2 (LRRK2) (4, 5), ubiquitin carboxyl terminal hydrolase-L1 (UCH-L1) (6), and α-synuclein (α-syn) (7, 8). Of these six genes, parkin, UCH-L1, α-syn, and DJ-1 are reported to have some relationship to the UPS. The loss of function mutation in parkin, an E3 ligase (9), causes autosomal recessive juvenile parkinsonism (AR-JP) (1). The I93M mutation in UCH-L1, an enzyme with both ubiquitin (Ub) hydrolase (10) and ligase (11) activities and a stabilizer of free mono Ub (12), is reported in autosomal dominant PD (6), while loss of UCH-L1 function is linked to neurodegenerative diseases distinct from PD (13). α-Syn, a small presynaptic protein without well-defined function (14), can become a substrate of parkin upon *O*-glycosylation (15). Missense mutations (7, 8) as well as whole gene triplication (16) of α-syn are reported in familial PD. Loss of function mutations in DJ-1, a cytoplasmic protein with multiple functions (17), are linked to AR-JP (2). Pathogenic mutants of DJ-1 are shown to specifically interact with parkin (18). Furthermore, in patients

*Corresponding author. FAX: +81-42-346-1745
E-mail: wada@ncnp.go.jp

with sporadic PD, decreased proteasomal activity is reported in the midbrain (19). Parkin (15), UCH-L1 (20), 26S proteasome (21), α-syn (22) as well as Ub (23) are found as the components of LB. Therefore, it has been assumed that insufficient function of the UPS plays an important role in the pathogenesis of PD.

Among the neurotoxins used to induce DA neurodegeneration, 6-hydroxy dopamine (6-OHDA), 1-methyl-4-phenyl-1,2,3,6-tetrahydropyridine (MPTP), and more recently, paraquate and rotenone have received most attention. Presumably, all of these toxins provoke the formation of reactive oxygen species (ROS). 6-OHDA was the first neurotoxin used to induce an animal model of PD associated with SNpc DA cell death (24). 6-OHDA-induced toxicity is relatively selective for monoaminergic neurons, resulting from preferential uptake by dopamine and noradrenaline transporters (25). 6-OHDA accumulates in the cytosol, resulting in the production of ROS, which inactivates biological macromolecules at their nucleophilic groups (26). The unilateral lesion by stereotaxic injection of 6-OHDA produces an asymmetric rotational behavior in the animals (27). The magnitude of rotation, which is quantitative, depends on the degree of the nigrostriatal lesion. Thus, this model has a notable advantage and is often used to assess anti-PD properties of drugs.

Inden et al. (28) unilaterally injected either 6-OHDA alone or in combination with proteasome inhibitors (PSI) to the mesencephalon of rats and examined the effect of PSI on DA cell death in vivo. Co-administration of lactacystin or MG-132 at relatively low doses with 6-OHDA (29) was shown to significantly reduce the rotational behavior. In some conditions, proteasome inhibition was able to rescue DA neurons from cell death. They further assessed the pathological changes in the substantia nigra and striatum of the rats. The loss of tyrosine hydroxylase (TH)-positive DA neurons as well as the reduction of TH-immunoreactive efferents in the striatum was significantly inhibited by the co-administration of PSI in 6-OHDA-injected rats. Besides, the co-administration of PSI with 6-OHDA significantly increased intracellular protein inclusions in surviving TH-positive neurons, which show α-syn and/or Ub immunoreactivities. The results by Inden et al. suggest the protective role of inclusion formation for 6-OHDA-induced DA cell death in the nigrostriatal region. In recent years, increasing evidences have indicated that inclusion formation is a mechanism of cells to intoxicate misfolded protein intermediates or oligomers and to compartmentalize them at the peri-nucleus (30, 31). The results by Inden et al. are in line with this indication.

The same group reported recently that 1-methyl-4-phenylpyridinium ion (MPP^+) treatment elevated both proteasome activity and DA cell death (32). However, co-administration of PSI blocked the effects of MPP^+ and increased α-syn-positive inclusions. Taken together, the two reports by the group are very intriguing because in their PD models, proteasome inhibition not only accelerated the inclusion formation but also prevented DA cell death. Furthermore, the reports brought up at least two important subjects that should be addressed to reveal the underlying mechanisms and to obtain effective therapeutic drugs for PD. The first issue is the target machinery of PSI. It has been known that inhibition of lysosomal enzymes by lactacystin and MG-132 is accompanied by some side effects (33). Recently, impairments in the autophagosome-lysosome system have been linked to some neurodegenerative diseases (34 – 38). The chaperon-mediated autophagic degradation of α-syn was reported and the pathogenic mutants of α-syn seem to gain toxic function in this pathway (39). Thus, further investigation of the functional link between UPS and the autophagosome-lysosome system should provide useful information for understanding the pathogenesis of PD. The second issue is the effect of PSI on DA neurons. Contradictory toxic effects of PSI on DA neurons have been reported by many groups (29, 40 – 42) Derangement of the UPS has been shown to result in neuronal cell death. Thus, it has been proposed that proteasomal dysfunction could be sufficient to induce DA cell death in the substantia nigra. However, most experiments were done using a relatively high dose of PSI. Recently, inhibition of the proteasome alone was shown to be insufficient to induce cell death, while the inhibition induced mitochondrial dysfunction or ROS formation (43). Furthermore, low-level of PSI exposure to SH-SY5Y cells was protective against serum withdrawal and oxidative stress (44). Together with the results by Inden et al. (28) and Sawada et al. (32) using PSI at low doses, the recent publications give us a cue to refine the link between UPS and the mechanisms of DA cell death. The effect of UPS inhibition might be harmful or beneficial, depending on the level of inhibition and other factors involved in DA cell maintenance. The precise features of the UPS in the pathogenesis of PD should be unveiled to seek effective drugs for this disease.

References

1 Kitada T, Asakawa S, Hattori N, Matsumine H, Yamamura Y, Minoshima S, et al. Mutations in the parkin gene cause autosomal recessive juvenile parkinsonism. Nature. 1998;392:605–608.

2 Bonifati V, Rizzu P, van Baren MJ, Schaap O, Breedveld GJ, Krieger E, et al. Mutations in the DJ-1 gene associated with autosomal recessive early-onset parkinsonism. Science. 2003;

299:256–259.
3 Valente EM, Abou-Sleiman PM, Caputo V, Muqit MM, Harvey K, Gispert S, et al. Hereditary early-onset Parkinson's disease caused by mutations in PINK1. Science. 2004;304:1158–1160.
4 Zimprich A, Biskup S, Leitner P, Lichtner P, Farrer M, Lincoln S, et al. Mutations in LRRK2 cause autosomal-dominant parkinsonism with pleomorphic pathology. Neuron. 2004;44:601–607.
5 Paisan-Ruiz C, Jain S, Evans EW, Gilks WP, Simon J, van der Brug M, et al. Cloning of the gene containing mutations that cause PARK8-linked Parkinson's disease. Neuron. 2004;44: 595–600.
6 Leroy E, Boyer R, Auburger G, Leube B, Ulm G, Mezey E, et al. The ubiquitin pathway in Parkinson's disease. Nature. 1998;395: 451–452.
7 Polymeropoulos MH, Lavedan C, Leroy E, Ide SE, Dehejia A, Dutra A, et al. Mutation in the alpha-synuclein gene identified in families with Parkinson's disease. Science. 1997;276:2045–2047.
8 Kruger R, Kuhn W, Muller T, Woitalla D, Graeber M, Kosel S, et al. Ala30Pro mutation in the gene encoding alpha-synuclein in Parkinson's disease. Nat Genet. 1998;18:106–108.
9 Shimura H, Hattori N, Kubo S, Mizuno Y, Asakawa S, Minoshima S, et al. Familial Parkinson disease gene product, parkin, is a ubiquitin-protein ligase. Nat Genet. 2000;25:302–305.
10 Larsen CN, Price JS, Wilkinson KD. Substrate binding and catalysis by ubiquitin C-terminal hydrolases: identification of two active site residues. Biochemistry. 1996;35:6735–6744.
11 Liu Y, Fallon L, Lashuel HA, Liu Z, Lansbury PT Jr. The UCH-L1 gene encodes two opposing enzymatic activities that affect alpha-synuclein degradation and Parkinson's disease susceptibility. Cell. 2002;111:209–218.
12 Osaka H, Wang YL, Takada K, Takizawa S, Setsuie R, Li H, et al. Ubiquitin carboxy-terminal hydrolase L1 binds to and stabilizes monoubiquitin in neuron. Hum Mol Genet. 2003;12: 1945–1958.
13 Saigoh K, Wang YL, Suh JG., Yamanishi T, Sakai Y, Kiyosawa H, et al. Intragenic deletion in the gene encoding ubiquitin carboxy-terminal hydrolase in gad mice. Nat Genet. 1999;23: 47–51.
14 Kahle PJ, Haass C, Kretzschmar HA, Neumann M. Structure /function of alpha-synuclein in health and disease: rational development of animal models for Parkinson's and related diseases. J Neurochem. 2002;82:449–457.
15 Shimura H, Schlossmacher MG, Hattori N, Frosch MP, Trockenbacher A, Schneider R, et al. Ubiquitination of a new form of alpha-synuclein by parkin from human brain: implications for Parkinson's disease. Science. 2001;293:263–269.
16 Singleton AB, Farrer M, Johnson J, Singleton A, Hague S, Kachergus J, et al. alpha-Synuclein locus triplication causes Parkinson's disease. Science. 2003;302:841.
17 Cookson MR. Pathways to Parkinsonism. Neuron. 2003;7:7–10.
18 Moore DJ, Zhang L, Troncoso J, Lee MK, Hattori N, Mizuno Y, et al. Association of DJ-1 and parkin mediated by pathogenic DJ-1 mutations and oxidative stress. Hum Mol Genet. 2005;14: 71–84.
19 McNaught KS, Jenner P. Proteasomal function is impaired in substantia nigra in Parkinson's disease. Neurosci Lett. 2001; 297:191–194.
20 Lowe J, McDermott H, Landon M, Mayer RJ, Wilkinson KD. Ubiquitin carboxyl-terminal hydrolase (PGP 9.5) is selectively present in ubiquitinated inclusion bodies characteristic of human neurodegenerative diseases. J Pathol. 1990;161:153–160.
21 Ii K, Ito H, Tanaka K, Hirano A. Immunocytochemical co-localization of the proteasome in ubiquitinated structures in neurodegenerative diseases and the elderly. J Neuropathol Exp Neurol. 1997;56:125–131.
22 Goedert M. Alpha-synuclein and neurodegenerative diseases. Nat Rev Neurosci. 2001;2:492–501.
23 Alves-Rodrigues A, Gregori L, Figueiredo-Pereira ME. Ubiquitin, cellular inclusions and their role in neurodegeneration. Trends Neurosci. 1998;21:516–520.
24 Ungerstedt U. 6-Hydroxy-dopamine induced degeneration of central monoamine neurons. Eur J Pharmacol. 1968;5:107–110.
25 Luthman J, Fredriksson A, Sundstrom E, Jonsson G, Archer T. Selective lesion of central dopamine or noradrenaline neuron systems in the neonatal rat: motor behavior and monoamine alterations at adult stage. Behav Brain Res. 1989;33:267–277.
26 Cohen G, Werner P. Free radicals, oxidative stress, and neurodegeneration. In: Neurodegenerative diseases. Calne BD editor. Philadelphia: WB Sanders; 1994. p. 139–161.
27 Ungerstedt U, Arbuthnott GW. Quantitative recording of rotational behavior in rats after 6-hydroxy-dopamine lesions of the nigrostriatal dopamine system. Brain Res. 1970;24:485–493.
28 Inden M, Kondo JI, Kitamura Y, Takata K, Nishimura K, Taniguchi T, et al. Proteasome inhibitors protect against degeneration of nigral dopaminergic neurons in hemiparkinsonian rats. J Pharmacol Sci. 2005;97:203–211.
29 McNaught KS, Bjorklund LM, Belizaire R, Isacson O, Jenner P, Olanow CW. Proteasome inhibition causes nigral degeneration with inclusion bodies in rats. Neuroreport. 2002;13:1437–1441.
30 Arrasate M, Mitra S, Schweitzer ES, Segal MR, Finkbeiner S. Inclusion body formation reduces levels of mutant huntingtin and the risk of neuronal death. Nature. 2004;431:805–810.
31 Ross CA, Pickart CM. The ubiquitin-proteasome pathway in Parkinson's disease and other neurodegenerative diseases. Trends Cell Biol. 2004;14:703–711.
32 Sawada H, Kohno R, Kihara T, Izumi Y, Sakka N, Ibi M, et al. Proteasome mediates dopaminergic neuronal degeneration, and its inhibition causes alpha-synuclein inclusions. J Biol Chem. 2004;279:10710–10719.
33 Lee DH, Goldberg AL. Proteasome inhibitors: valuable new tools for cell biologists. Trends Cell Biol. 1998;8:397–403.
34 Stefanis L, Larsen KE, Rideout HJ, Sulzer D, Greene LA. Expression of A53T mutant but not wild-type alpha-synuclein in PC12 cells induces alterations of the ubiquitin-dependent degradation system, loss of dopamine release, and autophagic cell death. J Neurosci. 2001;21:9549–9560.
35 Ravikumar B, Duden R, Rubinsztein DC. Aggregate-prone proteins with polyglutamine and polyalanine expansions are degraded by autophagy. Hum Mol Genet. 2002;11:1107–1117.
36 Webb JL, Ravikumar B, Atkins J, Skepper JN, Rubinsztein DC. Alpha-synuclein is degraded by both autophagy and the proteasome. J Biol Chem. 2003;278:25009–25013.
37 Fortun J, Dunn WA Jr, Joy S, Li J, Notterpek L. Emerging role for autophagy in the removal of aggresomes in Schwann cells. J Neurosci. 2003;23:10672–10680.
38 Simon D, Seznec H, Gansmuller A, Carelle N, Weber P, Metzger D, et al. Friedreich ataxia mouse models with progressive cerebellar and sensory ataxia reveal autophagic neuro-

degeneration in dorsal root ganglia. J Neurosci. 2004;24:1987–1995.

39 Cuervo AM, Stefanis L, Fredenburg R, Lansbury PT, Sulzer D. Impaired degradation of mutant alpha-synuclein by chaperone-mediated autophagy. Science. 2004;305:1292–1295.

40 Mytilineou C, McNaught KS, Shashidharan P, Yabut J, Baptiste RJ, Parnandi A, et al. Inhibition of proteasome activity sensitizes dopamine neurons to protein alterations and oxidative stress. J Neural Transm. 2004;11:1237–1251.

41 McNaught KS, Mytilineou C, Jnobaptiste R, Yabut J, Shashidharan P, Jennert P, et al. Impairment of the ubiquitin-proteasome system causes dopaminergic cell death and inclusion body formation in ventral mesencephalic cultures. J Neurochem. 2002;81:301–306.

42 McNaught KS, Perl DP, Brownell AL, Olanow CW. Systemic exposure to proteasome inhibitors causes a progressive model of Parkinson's disease. Ann Neurol. 2004;56:149–162.

43 Kikuchi S, Shinpo K, Tsuji S, Takeuchi M, Yamagishi S, Makita Z, et al. Effect of proteasome inhibitor on cultured mesencephalic dopaminergic neurons. Brain Res. 2003;964:228–236.

44 Ding Q, Dimayuga E, Martin S, Bruce-Keller AJ, Nukala V, Cuervo AM, et al. Characterization of chronic low-level proteasome inhibition on neural homeostasis. J Neurochem. 2003;86:489–497.

Available online at www.sciencedirect.com

SCIENCE DIRECT

Molecular Brain Research 126 (2004) 88–97

MOLECULAR BRAIN RESEARCH

www.elsevier.com/locate/molbrainres

Short communication

Microarray expression analysis of gad mice implicates involvement of Parkinson's disease associated UCH-L1 in multiple metabolic pathways

M. Bonin[a], S. Poths[a], H. Osaka[b], Y.-L. Wang[b], K. Wada[b], O. Riess[a,*]

[a] *Department of Medical Genetics, University of Tübingen, Calwerstrasse 7, 72076 Tübingen, Germany*

[b] *Department of Degenerative Neurological Diseases, National Institute of Neuroscience, NCNP, 4-1-1 Ogawahigashi, Kodaira, Tokyo 187-8502, Japan*

Accepted 9 March 2004

Abstract

Parkinson's disease (PD) is thought to be caused by environmental and genetic factors. Mutations in four genes, *α-synuclein*, *parkin*, *DJ-1*, and *UCH-L1*, have been identified in autosomal inherited forms of PD. The pathogenetic cause for the loss of neuronal cells in PD patients, however, remains to be determined. Due to the rarity of mutations in humans with PD, the analysis of animal models might help to further gain insights into the pathogenesis of familial PD. For UCH-L1, deficiency has been described in gad mice leading to axonal degeneration and formation of spheroid bodies in nerve terminals. Here, we investigated the gene expression pattern of the brain of 3-month-old Uch-l1-deficient gracile axonal dystrophy (*gad*) mice by microarray analysis. A total of 146 genes were differentially regulated by at least a 1.4-fold change with 103 being up-regulated and 43 being down-regulated compared with age and sex matched wildtype littermate mice. The gene products with altered expression are involved in protein degradation, cell cycle, vesicle transport, cellular structure, signal transduction, and transcription regulation. Most of the genes were modestly regulated, which is in agreement that severe alteration of these pathways might be lethal. Among the genes most significantly down-regulated is the brain-derived neurotrophic factor which might be one aspect of the pathogenesis in gad mice. Interestingly, several subunits of the transcription factor CCAAT/enhancer binding protein are up-regulated, which plays a central role in most altered pathways.

Theme: Disorders of the nervous system
Topic: Genetic models

Keywords: Ubiquitin; UCH-L1; Parkinson's disease; α-Synuclein; Protein degradation; Microarray chip analysis; Expression

1. Introduction

Parkinson's disease (PD) is the second most common neurodegenerative disorder in humans afflicting 1–2% of the population over 60 [6]. The leading clinical symptoms are mainly caused by loss of dopaminergic neurons of the SN. The cause of the neuronal cell death is not known yet but it is thought that genetic factors might be involved in a significant portion of the patients. In agreement with this assertion, increased concordance rates for PD were found in monozygotic twins (75%) vs. dizygotic twins (22%) [35]. Furthermore, numerous families with autosomal dominant inheritance of PD have been described [10,31,43]. Subsequently, mutations in the *α-synuclein* gene causing a rare autosomal dominant form of PD [18,36] have been described.

α-Synuclein is degraded by the ubiquitin–proteasome pathway [2,40]. Ubiquitin, a highly conserved 76 amino acid protein, is ligated through its C-terminus to the lysine side chains of proteins targeted for degradation by the 26S proteasome [4]. This process is catalyzed by a series of enzymes, called E1, E2, and E3. Mutations in one of the several hundreds of E3 ubiquitin ligases, which has been named parkin, cause an autosomal recessive form of early onset PD [17,26]. Parkin serves also as an E3 ligase [38] for a protein that interacts with α-synuclein and has been designated synphilin 1 [3]. Subsequently, we identified a mutation in synphilin-1 in PD patients [28]. An altered ubiquitin–proteasomal protein degradation pathway might therefore be

* Corresponding author. Tel.: +49-7071-29-76458; fax: +49-7071-29-5171.
E-mail address: olaf.riess@med.uni-tuebingen.de (O. Riess).

0169-328X/$ - see front matter © 2004 Elsevier B.V. All rights reserved.
doi:10.1016/j.molbrainres.2004.03.025

a key event in the pathogenesis of PD [19]. Efficient targeting for degradation by the 26S proteasome requires polyubiquitination. In addition to the isopeptide linkages made to lysines, the ubiquitin C-terminus can also form peptide bonds to α-linked polyubiquitin or ubiquitin followed by a C-terminal peptide extension [34]. This step is catalyzed by a family of Ubiquitin C-terminal hydrolases which are tissue-specific and likely to target distinct substrates. Of these, UCH-L1 is highly expressed in the brain [5,41] and has recently been implicated in PD by the identification of a missense mutation in autosomal dominant PD with reduced penetrance [20]. This I93M mutation was shown to decrease the hydrolytic activity in vitro significantly [20,32]. Although other genetic studies did not find the I93M mutation in further families, a S18Y polymorphism in UCH-L1 was found to be linked to a decreased susceptibility to PD [27,42]. Subsequently, Peter Lansbury's group has shown that the UCH-L1 gene encodes two opposing enzymatic activities indicating that UCH-L1 has an ubiquitin–ubiquitin ligase activity [23]. Inhibitors of the proteasomal pathway in cultured neurons by ubiquitin aldehyde which is a UCH inhibitor cause the formation of protein aggregates and cell death [30]. Most interestingly, UCH-L1 is also part of the Lewy bodies [25].

Although evidence for an altered ubiquitin–proteasomal protein degradation pathway as the cause of PD is striking, the cause of the selective degeneration of dopaminergic neurons in PD patients has not been elucidated. We thought to gain insight into the complex metabolic pattern of neurons by investigating UCH-L1-deficient gracile axonal dystrophy (*gad*) mice using microarray expression analyses. The *gad* mouse is an autosomal recessive spontaneous neurological mutant that was identified in 1984 [37]. Our positional cloning approach successfully identified that the gad mutation is caused by an intragenic deletion of the *Uch-l1* gene including exons 7 and 8 [37]. Subsequent studies have shown that the mutant lacks the expression of UCH-L1 protein [33,37]. Pathologically, the *gad* mouse displays dying-back type of axonal degeneration of the gracile tract. Most interestingly, *gad* mice develop accumulation of amyloid precursor protein (APP) in form of ubiquitin-positive deposits along the sensory and motor nervous systems staining [13], another indication that the gad mutation affects protein turnover. Therefore, direct involvement of an altered ubiquitin system in neurodegeneration has been indicated by this model.

2. Methods

2.1. Mice

Three-month-old male homozygous Uch-l1 deficient (*gad*) mice and their age and sex matched wildtype littermate mice (CBA/RFM) were analyzed in the microarray analysis. Mice were maintained and propagated at National Institute of Neuroscience, National Center of Neurology and Psychiatry (Japan). Experiments using these mice were approved by the Animal Investigation Committee of the Institute.

2.2. Brain tissue preparation and RNA analysis

Mice were killed by cervical dislocation, brains were quickly removed, immersed briefly in ice-cold saline, and whole brains were frozen on dry ice and stored at −80 °C. Total RNA was extracted from mouse whole brain including olfactory bulb, cerebellum and brain stem by using RNeasy kits (Qiagen). The RNA quality was controlled by Lab-on-Chip-System Bioanalyser 2100 (Agilent).

2.3. Microarray analysis

Double-stranded cDNA was synthesized from the total RNA of one whole brain using a Superscript choice kit (Invitrogen) with a T7-(dT)24 primer incorporating a T7 RNA polymerase promoter (Metabion). cRNA was prepared and biotin labeled by in vitro transcription (Enzo Biochemical). Labeled RNA was fragmented by incubation at 94 °C for 35 min in the presence of 40 mM Tris-OAc (pH 8.1), 100 mM KOAc, and 30 mM MgOAc. Labeled, fragmented cRNA (15 μg) was hybridized for 16 h at 45 °C to a MG-U74A mouse genome array (Affymetrix). After hybridization, gene chips were automatically washed and stained with streptavidin–phycoerythrin using a fluidics station. The probe arrays were scanned at 3-μm resolution using a Genechip System confocal scanner made for Affymetrix by Agilent.

Affymetrix Microarray Suite software (version 5.0), MicroDB and Data Mining Tool were used to scan and analyze the relative abundance of each gene based on the intensity of the signal from each probe set. Analysis parameters used by the software were set to values corresponding to moderate stringency (statistical difference threshold = 30, statistical ratio threshold = 1.5). Output from the microarray analysis was merged with the Unigene or GenBank descriptor and saved as an Excel data spreadsheet.

Each cRNA generated from a brain was hybridized on one microarray separately. We ran three arrays analyzing three gad mice vs. two controls allowing a total of six comparisons (3 × 2 matrix). For each comparison, the analysis using the Affymetrix software generates a "difference call" of no change, marginal increase/decrease, or increase/decrease, respectively. Only those genes which were found in at least six of six comparisons similarly adjusted were defined as stringent differentially expressed genes. Genes which were found in five of six comparisons similarly adjusted were defined as moderate differentially expressed genes. The magnitude and direction of expression changes were estimated as Signal Log Ratio (SLR). The log scale used is base 2, making it intuitive to interpret the Signal Log Ratios in terms of multiples of two. Thus, an SLR of 1.0 indicates an increase of the transcript level by two-fold and −1.0 indicates a two-fold decrease. An SLR

Table 1a
List of stringent differentially regulated genes

GenBank ID	slr—Average	slr—S.D.	Gene-information
RNA-metabolism (3)			
AA791742	1.09	0.28	ARP2 actin-related protein 2 homolog (yeast)
AA690583	0.87	0.34	splicing factor proline/glutamine rich (polypyrimidine tract binding protein associated)
AI843586	0.72	0.21	splicing factor, arginine/serine rich 9 (25 kDa)
Vesicle-transport-proteins (3)			
U60150	0.8	0.24	vesicle-associated membrane protein 2
AB025218	0.71	0.11	coated vesicle membrane protein
D12713	0.68	0.15	SEC23A (*S. cerevisiae*)
Cellular structure proteins (4)			
AF067180	1	0.16	kinesin family member 5C
AB023656	0.6	0.21	kinesin heavy chain member 1B
M21041	0.73	0.21	microtubule-associated protein 2
M18775	−0.69	0.22	microtubule-associated protein tau
Channel-proteins (4)			
X78874	0.81	0.19	chloride channel 3
X16645	0.74	0.28	ATPase, Na+/K+ transporting, beta 2 polypeptide
U14419	0.67	0.14	gamma-aminobutyric acid (GABA-A) receptor, subunit beta 2
U16959	0.65	0.15	FK506 binding protein 5 (51 kDa)
Defense (2)			
X06454	0.73	0.24	complement component 4 (within H-2S)
X66295	0.53	0.11	complement component 1, q subcomponent, c polypeptide
Ca-metabolism (2)			
X87142	0.83	0.33	calcium/calmodulin-dependent protein kinase II alpha
AI842328	0.82	0.58	calmodulin 3
Growth factors (1)			
X55573	−0.73	0.23	brain-derived neurotrophic factor
Chaperones (1)			
M20567	0.97	0.31	heat shock protein, 70 kDa 2
Signal transduction (13)			
U50413	1.53	0.92	phosphatidylinositol 3-kinase, regulatory subunit, polypeptide 1 (p85 alpha)
AF022992	1.04	0.13	period homolog 1 (*Drosophila*)
AI838022	0.89	0.31	ADP-ribosylation factor 3
AI849333	0.75	0.17	cerebellar postnatal development protein 1
X84239	0.74	0.14	RAB5B, member RAS oncogene family
AW125157	0.7	0.1	F-box and WD-40 domain protein 1B
AB005654	0.7	0.14	mitogen-activated protein kinase kinase 7
M97516	0.69	0.11	
AA822412	0.68	0.27	RIKEN cDNA 2610313E07 gene

Table 1a (*continued*)

GenBank ID	slr—Average	slr—S.D.	Gene-information
Signal transduction (13)			
AF001871	0.66	0.13	pleckstrin homology, Sec7 and coiled/coil domains 3
D87902	0.62	0.17	ADP-ribosylation factor 5
AI840130	−0.56	0.15	Src activating and signaling molecule
AV280750	−0.56	0.14	mitogen-activated protein kinase 10
Protein degradation (10)			
AW125800	1.18	0.35	ESTs, weakly similar to ubiquitin specific protease 8; putative deubiquitinating enzyme [*Mus musculus*] [*M. musulus*]
L21768	0.83	0.13	epidermal growth factor receptor pathway substrate 15
X57349	0.65	0.11	transferrin receptor
AW050342	0.5	0.09	ubiquitin specific protease 21
AI849361	−0.54	0.12	RIKEN cDNA 1700056O17 gene
AI838853	−0.59	0.08	ubiquitin carboxyl-terminal esterase L5
AI839363	−0.65	0.17	eukaryotic translation initiation factor 3, subunit 6 48-kDa
AI846787	−0.67	0.22	Vhlh-interacting deubiquitinating enzyme 1
AI842835	−0.7	0.09	RIKEN cDNA 1500004O06 gene
AI839225	−0.86	0.17	leucine aminopeptidase 3
Membrane-transport (4)			
AF064748	1.56	0.7	plasma membrane associated protein, S3-12
M22998	1.13	0.27	solute carrier family 2 (facilitated glucose transporter), member 1
M75135	0.89	0.32	solute carrier family 2 (facilitated glucose transporter), member 3
AI843448	0.84	0.36	microsomal glutathione *S*-transferase 3
Transcription-regulation (12)			
M36514	1.19	0.26	zinc finger protein 26
AB021491	0.92	0.32	staphylococcal nuclease domain containing 1
M61007	0.96	0.23	CCAAT/enhancer binding protein (C/EBP), beta
M62362	0.81	0.04	CCAAT/enhancer binding protein (C/EBP), alpha
AI850638	0.65	0.13	thyrotroph embryonic factor
U47543	0.62	0.23	Ngfi-A binding protein 2
X61800	0.51	0.14	CCAAT/enhancer binding protein (C/EBP), delta
U16322	−0.56	0.1	transcription factor 4
AF034745	−0.63	0.17	ligand of numb-protein × 1
Z67747	−0.65	0.13	zinc finger protein 62
AI843959	−0.66	0.25	RIKEN cDNA 5730403B10 gene
X94127	−0.94	0.14	SRY-box containing gene 2
Others and non-classified (21)			
AI851703	1.31	0.47	expressed sequence AW049671
AW227650	1.25	0.26	RIKEN cDNA 0610038P07 gene
AI877157	1.21	0.41	transmembrane 4 superfamily member 9
AF058799	1.14	0.31	3-monooxgenase/tryptophan 5-monooxgenase activation protein, gamma polypeptide

Table 1a (*continued*)

GenBank ID	slr—Average	slr—S.D.	Gene-information
Others and non-classified (21)			
X02801	1	0.53	glial fibrillary acidic protein
D85785	0.92	0.07	protein tyrosine phosphatase, non-receptor type substrate 1
U75321	0.72	0.32	ATPase, aminophospholipid transporter (APLT), class I, type 8A, member 1
AF042180	0.67	0.17	testis-specific protein, Y-encoded-like
AW124835	0.59	0.05	similar to *S*-adenosylmethionine synthetase gamma form (Methionine adenosyltransferase) (AdoMet synthetase) (MAT-II)
AI835481	0.57	0.15	beta-1,3-glucuronyltransferase 3 (glucuronosyltransferase I)
AB033168	0.56	0.23	ZAP3 protein
U51167	0.56	0.03	isocitrate dehydrogenase 2 (NADP+), mitochondrial
X66091	0.54	0.08	*M. musculus* ASF mRNA
AW212859	−0.53	0.12	axotrophin
AI843662	−0.53	0.2	stromal membrane-associated protein
AW046672	−0.53	0.08	DNA segment, Chr 11, ERATO Doi 603, expressed
L00993	−0.53	0.13	Sjogren syndrome antigen B
AW124329	−0.54	0.14	RIKEN cDNA 4921531G14 gene
AI844469	−0.56	0.13	RIKEN cDNA 0610012D09 gene
M34896	−0.56	0.14	ecotropic viral integration site 2
U95498	−0.67	0.22	ALL1-fused gene from chromosome 1q

of zero would indicate no change. Categorization was based on the NetAffx database (http://www.NetAffx.com) [22]. For unsupervised, hierarchical cluster analysis, the Genesis software was used [39].

3. Results

In order to gain insight into the complex expression pattern of mice with a disturbed protein degradation pathway, microarrays representing 12,000 genes were hybridized with labelled RNA isolated from whole brain tissue of 3-month-old male gad mice and compared to two wildtype littermates of the same age. Thus, six comparisons of the expression pattern were achieved. The complete raw data set is publicly available and can be requested directly from the authors. We called a gene (a) stringent differentially regulated when at least six of the six comparisons revealed similar results or (b) moderate differentially regulated when five of six comparisons showed similar results. For both stringencies, genes with an expression difference of at least 1.4-fold (Signal Log Ratio of 0.5) between gad and wildtype mice were considered as significant.

The criteria for stringent differentially regulated genes (Table 1a) were fulfilled by 76 genes with known or putative function and by four ESTs with unknown function. Fifty seven of the genes were up-regulated, whereas

Table 1b
List of moderate differentially regulated genes

GenBank ID	slr—Average	slr—S.D.	Gene-information
RNA-metabolism (4)			
AA791742	1.09	0.28	ARP2 actin-related protein 2 homolog (yeast)
AA690583	0.87	0.34	splicing factor proline/glutamine rich (polypyrimidine tract binding protein associated)
U93050	0.77	0.43	poly(A) binding protein, nuclear 1
AI843586	0.72	0.21	splicing factor, arginine/serine rich 9 (25 kDa)
Vesicle-transport-proteins (4)			
U60150	0.8	0.24	vesicle-associated membrane protein 2
AB025218	0.71	0.11	coated vesicle membrane protein
D12713	0.68	0.15	SEC23A (*S. cerevisiae*)
U91933	0.64	0.3	adaptor-related protein complex AP-3, sigma 2 subunit
Cellular structure proteins (6)			
AF067180	1	0.16	kinesin family member 5C
U51204	0.6	0.19	expressed sequence AI790651
AB023656	0.6	0.21	kinesin heavy chain member 1B
M21041	0.73	0.21	microtubule-associated protein 2
X61399	0.69	0.4	MARCKS-like protein
M18775	−0.69	0.22	microtubule-associated protein tau
Channel-proteins (10)			
X78874	0.81	0.19	chloride channel 3
X16645	0.74	0.28	ATPase, Na+/K+ transporting, beta 2 polypeptide
U43892	0.7	0.16	ATP-binding cassette, subfamily B (MDR/TAP), member 7
U14419	0.67	0.14	gamma-aminobutyric acid (GABA-A) receptor, subunit beta 2
Y17393	0.66	0.24	prefoldin 2
U16959	0.65	0.15	FK506 binding protein 5 (51 kDa)
D10028	0.55	0.2	glutamate receptor, ionotropic, NMDA1 (zeta 1)
D50032	0.51	0.2	trans-golgi network protein 2
U73625	0.51	0.11	transient receptor potential cation channel, subfamily C, member 1
Defense (3)			
X06454	0.73	0.24	complement component 4 (within H-2S)
AW050268	0.64	0.19	HLA-B associated transcript 2
X66295	0.53	0.11	complement component 1, q subcomponent, c polypeptide
Lipid-metabolism (3)			
M91458	−0.53	0.7	sterol carrier protein 2, liver
AB017026	−0.54	0.19	oxysterol binding protein-like 1A
AI845798	−0.6	0.35	RIKEN cDNA 2310004B05 gene
Ca-metabolism (2)			
X87142	0.83	0.33	calcium/calmodulin-dependent protein kinase II alpha
AI842328	0.82	0.58	calmodulin 3
Growth factors (2)			
U42384	−0.65	0.25	fibroblast growth factor inducible 15
X55573	−0.73	0.23	brain-derived neurotrophic factor

(continued on next page)

Table 1b (*continued*)

GenBank ID	slr	Average slr	S.D.	Gene-information
Chromatin-structure (2)				
M25773	0.7	0.33		SWI/SNF related, matrix associated, actin-dependent regulator of chromatin, subfamily d, member 1
AA794509	0.64	0.27		SWI/SNF-related, matrix-associated, actin-dependent regulator of chromatin, subfamily a, member 5
Chaperones (2)				
D85904	−0.56	0.16		heat shock 70 kDa protein 4
M20567	0.97	0.31		heat shock protein, 70 kDa 2
Signal transduction (25)				
U50413	1.53	0.92		phosphatidylinositol 3-kinase, regulatory subunit, polypeptide 1 (p85 alpha)
AF077660	1.26	0.23		homeodomain interacting protein kinase 3
AF022992	1.04	0.13		period homolog 1 (*Drosophila*)
AI838022	0.89	0.31		ADP-ribosylation factor 3
M63659	0.88	0.46		guanine nucleotide binding protein, alpha 12
U29055	0.77	0.32		guanine nucleotide binding protein, beta 1
AI849333	0.75	0.17		cerebellar postnatal development protein 1
X84239	0.74	0.14		RAB5B, member RAS oncogene family
AW125157	0.7	0.1		F-box and WD-40 domain protein 1B
AB005654	0.7	0.14		mitogen-activated protein kinase kinase 7
AI645561	0.69	0.28		NMDA receptor-regulated gene 1
M97516	0.69	0.11		
AA822412	0.68	0.27		RIKEN cDNA 2610313E07 gene
AF001871	0.66	0.13		pleckstrin homology, Sec7 and coiled/coil domains 3
AA982714	0.64	0.36		adrenergic receptor kinase, beta 1
AF054623	0.62	0.17		frizzled homolog 1, (*Drosophila*)
D87902	0.62	0.17		ADP-ribosylation factor 5
AF014371	0.61	0.18		ras homolog gene family, member A2
AI450876	0.59	0.17		*Mus musculus*, similar to pyridoxal kinase, clone MGC:29261 IMAGE:5064695, mRNA, complete cds
AJ001418	0.57	0.1		pyruvate dehydrogenase kinase, isoenzyme 4
L25674	0.56	0.19		nuclear receptor subfamily 2, group F, member 6
AI840130	−0.56	0.15		Src activating and signaling molecule
AV280750	−0.56	0.14		mitogen-activated protein kinase 10
U20238	−0.56	0.12		RAS p21 protein activator 3
AV370035	−0.73	0.23		chemokine (C–C) receptor 5
Protein degradation (12)				
AW125800	1.18	0.35		ESTs, weakly similar to ubiquitin specific protease 8; putative deubiquitinating enzyme [*Mus musculus*] [*M. musulus*]
L21768	0.83	0.13		epidermal growth factor receptor pathway substrate 15

Table 1b (*continued*)

GenBank ID	slr	Average slr	S.D.	Gene-information
Protein degradation (12)				
AI853269	0.66	0.27		proteasome (prosome, macropain) subunit, beta type 2
X57349	0.65	0.11		transferrin receptor
M97216	0.59	0.28		amyloid beta (A4) precursor-like protein 2
AW050342	0.5	0.09		ubiquitin specific protease 21
AI849361	−0.54	0.12		RIKEN cDNA 1700056O17 gene
AI838853	−0.59	0.08		ubiquitin carboxyl-terminal esterase L5
AI839363	−0.65	0.17		eukaryotic translation initiation factor 3, subunit 6 48-kDa
AI846787	−0.67	0.22		Vhlh-interacting deubiquitinating enzyme 1
AI842835	−0.7	0.09		RIKEN cDNA 1500004O06 gene
AI839225	−0.86	0.17		leucine aminopeptidase 3
Membran-transport (5)				
AF064748	1.56	0.7		plasma membrane associated protein, S3−12
M22998	1.13	0.27		solute carrier family 2 (facilitated glucose transporter), member 1
AB035174	1.03	0.48		sialytransferase 7 ((alpha-*N*-acetylneuraminyl 2,3-betagalactosyl-1,3)-*N*-acetyl galactosaminide alpha-2, 6-sialytransferase) F
M75135	0.89	0.32		solute carrier family 2 (facilitated glucose transporter), member 3
AI843448	0.84	0.36		microsomal glutathione *S*-transferase 3
Transcription-regulation (22)				
M36514	1.19	0.26		zinc finger protein 26
AB021491	0.92	0.32		staphylococcal nuclease domain containing 1
M88299	1.11	0.5		
M61007	0.96	0.23		CCAAT/enhancer binding protein (C/EBP), beta
M62362	0.81	0.04		CCAAT/enhancer binding protein (C/EBP), alpha
AF015881	0.73	0.13		
AI850638	0.65	0.13		thyrotroph embryonic factor
U47543	0.62	0.23		Ngfi-A binding protein 2
AF064553	0.58	0.25		nuclear receptor-binding SET-domain protein 1
AF084480	0.54	0.19		bromodomain adjacent to zinc finger domain, 1B
X61800	0.51	0.14		CCAAT/enhancer binding protein (C/EBP), delta
X72310	−0.5	0.18		transcription factor Dp 1
L10426	−0.52	0.24		ets variant gene 1
D38046	−0.55	0.19		topoisomerase (DNA) II beta
U16322	−0.56	0.1		transcription factor 4
U07861	−0.59	0.15		zinc finger protein 101
AF034745	−0.63	0.17		ligand of numb-protein × 1
Z67747	−0.65	0.13		zinc finger protein 62
AI843959	−0.66	0.25		RIKEN cDNA 5730403B10 gene
AI957030	−0.66	0.33		RIKEN cDNA 2310001H12 gene
AI851230	−0.76	0.12		RIKEN cDNA 2310035M22 gene
X94127	−0.94	0.14		SRY-box containing gene 2

Table 1b (*continued*)

GenBank ID	slr—Average	slr—S.D.	Gene-information
Others and non-classified (44)			
AI851703	1.31	0.47	expressed sequence AW049671
AW227650	1.25	0.26	RIKEN cDNA 0610038P07 gene
AI877157	1.21	0.41	transmembrane 4 superfamily member 9
AF058799	1.14	0.31	3-monooxgenase/tryptophan 5-monooxgenase activation protein, gamma polypeptide
X02801	1	0.53	glial fibrillary acidic protein
D85785	0.92	0.07	protein tyrosine phosphatase, non-receptor type substrate 1
M93310	0.86	0.76	metallothionein 3
U52824	0.81	0.17	tubby
AI646638	0.79	0.15	*Mus musculus*, clone MGC:37615 IMAGE:4989784, mRNA, complete cds
AF006466	0.79	0.03	formin-like
AW227650	0.77	0.22	RIKEN cDNA 0610038P07 gene
U75321	0.72	0.32	ATPase, aminophospholipid transporter (APLT), class I, type 8A, member 1
AF039833	0.69	0.39	contactin associated protein 1
AF042180	0.67	0.17	testis-specific protein, Y-encoded-like
U62673	0.62	0.12	
AI849718	0.6	0.2	RIKEN cDNA 1500010B24 gene
AA414964	0.6	0.2	ESTs, Weakly similar to ATY1_MOUSE Probable cation-transporting ATPase 1 [*M. musulus*]
AW124835	0.59	0.05	similar to *S*-adenosylmethionine synthetase gamma form (Methionine adenosyltransferase) (AdoMet synthetase) (MAT-II)
AF076482	0.57	0.17	peptidoglycan recognition protein
AI835481	0.57	0.15	beta-1,3-glucuronyltransferase 3 (glucuronosyltransferase I)
AB033168	0.56	0.23	ZAP3 protein
U51167	0.56	0.03	isocitrate dehydrogenase 2 (NADP+), mitochondrial
AW124101	0.55	0.08	expressed sequence AA408278
X66091	0.54	0.08	*M. musculus* ASF mRNA
U11075	0.54	0.13	potassium inwardly-rectifying channel, subfamily J, member 4
D00472	0.51	0.15	cofilin 1, non-muscle
AJ006587	0.5	0.16	eukaryotic translation initiation factor 2, subunit 3, structural gene X-linked
AW048159	0.5	0.1	RIKEN cDNA 1200017E04 gene
AW212859	−0.53	0.12	axotrophin
AI843662	−0.53	0.2	stromal membrane-associated protein
AW046672	−0.53	0.08	DNA segment, Chr 11, ERATO Doi 603, expressed
L00993	−0.53	0.13	Sjogren syndrome antigen B
AW124044	−0.53	0.06	protein-L-isoaspartate (D-aspartate) *O*-methyltransferase 1
AW124329	−0.54	0.14	RIKEN cDNA 4921531G14 gene
AA839379	−0.55	0.14	RIKEN cDNA 2610002J02 gene
AI504338	−0.56	0.2	ESTs
AI844469	−0.56	0.13	RIKEN cDNA 0610012D09 gene
M34896	−0.56	0.14	ecotropic viral integration site 2
U83174	−0.57	0.22	gene trap ROSA 26, Philippe Soriano
AI853444	−0.59	0.22	RIKEN cDNA 2610042L04 gene
AA623587	−0.6	0.1	expressed sequence AA536743
U95498	−0.67	0.22	ALL1-fused gene from chromosome 1q

23 genes were down-regulated in the *gad* mice. These genes can be grouped according to their function (Table 1a) into RNA metabolism (3 up- and 0 down-regulated, 3/0), vesicle transport (3/0), proteins of the cell structure (3/1), channel proteins (4/0), calcium metabolism (2/0), growth factors (0/1), chaperones (1/0), signal transduction (11/2), membrane transport (4/0), transcription regulation (7/5), and others or unknown function (13/8). Nearly no gene of the immune-related proteins was found to be differentially regulated (2/0).

The criteria for moderate regulated genes were fulfilled by 134 genes with known or putative function and 12 ESTs without known function. A total of 103 of the genes were up-regulated, whereas 43 genes were down-regulated in the *gad* mice. These genes can be grouped according to their function (Table 1b) into RNA metabolism (4 up- and 0 down-regulated, 4/0), vesicle transport (4/0), proteins of the cell structure (5/1), defense (3/0), channel proteins (10/0), Lipid metabolisms (0/3), calcium metabolism (2/0), growth factors (0/2), chromatin structure (2/0), chaperones (1/1), signal transduction (21/4), membrane transport (5/0), transcription regulation (11/11), and others or unknown function (30/14).

Of the protein degradation pathway, six genes were down-regulated and another four genes were found to be up-regulated (Table 1a). Our first hypothesis that genes of the UCH gene family might compensate for the lack of UCH-L1 function was not confirmed. In contrast, UCH-L5 was found to be down-regulated.

At a first look, UCH-L1 was not differentially expressed. The reduction of the signal by the deletion of exons 7 and 8 is too weak for a change call of the Affymetrix software. However, the appropriate oligos show the absence of the corresponding RNA regions (data not shown).

An unsupervised, hierarchical cluster algorithm allowed us to cluster the five analyzed brains on the basis of their similarities measured over these 146 significant regulated genes from Table 1b (Fig. 1). In the dendrogram shown in Fig. 1 (left and top), the length and the subdivision of the branches display the relatedness of the brains (top) and the expression of the genes (left). Two distinct groups of brains (3 KO and 2 wt brains) and two groups of genes are shown.

4. Discussion

Ubiquitin has been implicated in numerous processes of the cell including cell-cycle control, receptor function,

Fig. 1. Unsupervised two-dimensional cluster analysis of transcript ratios for the five mice brains (3 KO and 2 wt brains). There were 146 significant genes across the group. Each row represents a single gene and each column one brain. As shown in the colour bar, red indicates up-regulation, green down-regulation, black no change, and grey no data available.

signalling pathways, antigen presentation, degradation of proteins, and regulation of transcription. Analogous to these functions, alteration of the ubiquitin pathway will affect several of these pathways which may not be identifiable by single gene analysis. To investigate the complex network of gene regulation, we analyzed the expression pattern of 12,000 genes in 3-month-old male Uch-l1 deficient (*gad*) mice. This age was described to present the progressive phase of the disease [13]. The mutant mice used for this study showed sensory ataxia and motor paresis. Significant expression changes were found in more then 146 genes (Tables 1a and b). As expected, these genes are involved in several pathways of protein degradation, transcription regulation, vesicle and membrane transport, and signal transduction.

The gene most significantly down-regulated in the gad mice was Sox2 also known as SRY-box containing gene 2 (Signal log ratio −0.94, S.D. 0.14). Mutations of SOX2 cause anophthalmia in humans [9]. In mice, inactivation of Sox2 suggested a role in embryonal implantation [1]. SOX2

has been implicated in the regulation of Fgf4 expression [1]. In our experiments, we found no indication for a differential regulation of Fgf4, however, the inducible Fgf15 was down-regulated in *gad* mice (−0.65, S.D. 0.25) suggesting a role of Sox2 in Fgf15 expression and indicating a complex expression regulation mechanism of the Fgf gene family. Fgfs have been defined as regulators of the central nervous development and function (reviewed in Ref. [7]). However, the functional implication of a down-regulation of Fgf15 in mice has not been explored yet. Therefore, gad mice might suit as a model to study Fgf15 in more detail. Cofactors of Sox2 are totally unknown. One could speculate that transcription factors acting partially synergistic with Sox2 might be up-regulated in gad mice. In fact, we found several up-regulated transcription factors such as the eukaryotic translation initiation factor 2 (0.5, S.D. 0.16), the zinc finger protein 26 (1.19, S.D. 0.26), and CCAAT/enhancer binding protein (0.96, S.D. 0.23), respectively. Most convincingly, mRNAs of the alpha, beta, and delta subunits of the CCAAT/enhancer binding protein (C/EBP) were increased, respectively. Fig. 2 shows the central role of C/EBP. More than 20 adjusted genes can be implemented on a coherent biochemical network. For example, C/EBPs provide another link to the above-mentioned Fgf expression changes as a C/EBP site is an important regulatory element for FGF-binding protein activity [14]. Early changes of expression of C/EBP beta were also observed in other neurodegenerative diseases [21]. Most interestingly, only the inhibitory gamma and zeta subunits of C/EBP but not the positively functioning beta subunit have been found to be multi-ubiquinated and degraded by the proteasome [11]. We also found mRNA encoding the homeodomain interacting protein kinase 3 (HIPK3) to be up-regulated (1.26, S.D. 0.23). HIPK3 belongs to a family of co-repressors that potentiate the transcriptional activities of homeoproteins [16]. In gad mice, we found the homeobox gene containing transcription factor paired box gene 6 down-regulated (−0.44, S.D. 0.12). However, whether interaction of HIPK3 to the paired box gene 6 or other transcription factors as Sox2 is part of transcription activation has not been shown yet. Interestingly though, mutations in the paired box gene 6 causes eye diseases as mutations in Sox 2 [9]. How UCH-L1 is implicated in this process needs to be defined. For gad mice, however, abnormal eye development has not been described. It is likely that complete loss of function but no small alterations of the expression levels of these genes lead to the described developmental alterations. In gad mice, several other transduction pathways seem to be altered including the phosphatidylinositol 3 kinase (PI3K) pathway which is also linked to C/EBP. Specifically, the p85 alpha subunit of PI3K was found to be up-regulated (1.53; S.D. 0.92) (Fig. 2).

Besides the above-mentioned reduction of fgf15 mRNA, the brain-derived neurotrophic factor (BDNF) is also reduced in gad mice (−0.73, S.D. 0.23). BDNF has been reported to act on motor neurons [12] and to stimulate developmental neuro-muscular synapses [24]. Although BDNF reduction has not been reported yet in gad mice, one of us found significantly reduced NGF levels primarily in the spinal cord but not in the brain [29]. It has to be mentioned that spinal cord was not analyzed in our Chip analyses. However, in gad mice, decreased muscle weight has been observed with age which could be caused by the reduced BDNF and/or fgf15 levels, respectively. Although the function of another trophin, axotrophin, needs still to be explored, a reduction (−0.53, S.D. 0.12) of this factor implicates its significance in neuronal survival. In agreement with this hypothesis, Haendel and colleagues found neuronal degeneration in axotrophin-deficient mice (NCBI link NM_020575). In contrast, epidermal growth factor

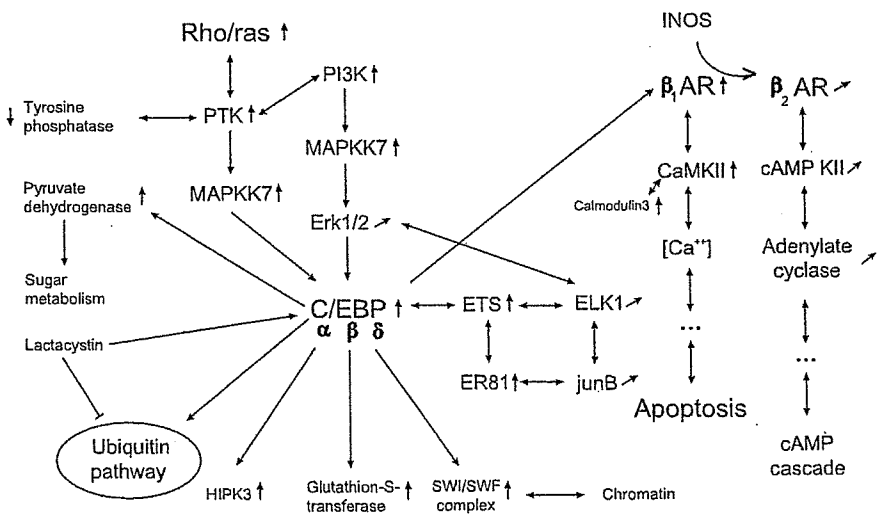

Fig. 2. C/EBP pathway demonstrating interactions of proteins which transcripts are differentially regulated in gad mice (up-regulated in six of six comparisons marked with ↑, upregulated genes in five or six of six comparisons are indicated with /, down-regulated in six of six comparisons are indicated with ↓).

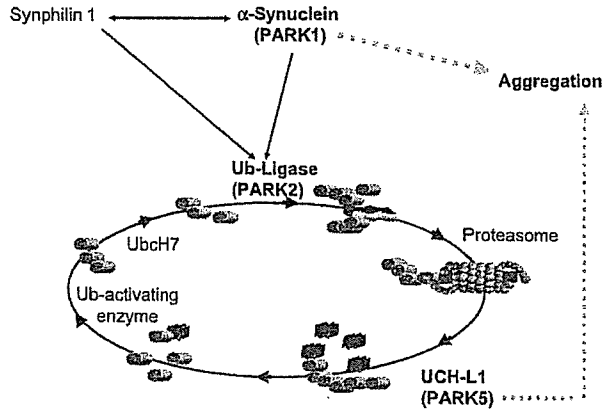

Fig. 3. Scheme of proteins altered in Parkinson's disease which place UCH-L1 as part of the altered protein degradation pathway and highlight the role of investigating Uch-l1-deficient (gad) mice by expression analysis.

receptor pathway substrate 15 was increased (0.83, S.D. 0.13) and might indicate a regulatory mechanism of gad mice trying to prevent neuronal degeneration.

Pathological features of gad mice are spheroid dystrophic axons dying back the dorsal root ganglia (DRG) progressing along the gracile tract of the spinal cord towards the parental neurons [15]. Immunohistochemically, almost all of the primary neurons and of the glial cells in DRG of gad mice revealed strong amyloid precursor protein (APP) staining [13]. The authors hypothesized abnormal expression of APP in gad mice as the cause of the pathological features. Although increased APP transcript in the brain has not been confirmed by our transcription analysis, amyloid beta (A4) precursor-like protein 2 was upregulated (0.59, S.D. 0.28). Our data also define an up-regulation of glial fibrillary acidic protein (GFAP) as the cause of the increased immunoreactivity of GFAP in astrocytes of gad mice [44].

We were in particular interested in genes involved in protein degradation. We hypothesized to find genes encoding proteins with UCH-L1 complementary functions compensatory up-regulated. Fig. 3 shows a simplified scheme of ubiquitin-altered protein degradation in PD and the task of UCH-L1. However, only the beta type 2 proteasome (prosome, macropain) subunit (0.66, S.D. 0.27) and the ubiquitin specific protease 21 (0.5, S.D. 0.09) were found to be increased. Interestingly, ubiquitin C-terminal hydrolase activity is associated with the 26S protease complex [8]. However, a direct interaction between UCH-L1 and macropain remains to be shown. Furthermore, Hsp70 protein 2 was increased (0.97, S.D. 0.31) likely due to decreased proteasomal degradation of proteins in gad mice, whereas Hsp70 protein 4 was down-regulated (−0.56, S.D. 0.16). Ubiquitin carboxyl-terminal esterase L5 was also significantly decreased (−0.59, S.D. 0.08).

In summary, the alteration of many pathways in gad mice offers an interesting mouse model which needs to be studied in more detail. The development of genome wide transcription profiles of mouse models in general will help to decipher the interaction and dependence of genes and gene products in their complexity of a living organism. Although it is not clear yet whether this complexity of biology in development, health and disease into their final details will be completely understood, a first step is being done to explore normal variation and disease processes at the RNA level using microarray chip analyses.

Acknowledgements

The authors thank D. Berg for the helpful discussions. This work was supported by a grant from the Federal Ministry of Education and Research (Fö. 01KS9602) and the Interdisciplinary Center of Clinical Research Tübingen (IZKF). Work of K.W. was supported by the grant for Research on Brain Science from the Ministry of Health, Labour and Welfare of Japan, Grants-in-Aid for Scientific Research from the Ministry of Education, Culture, Sports, Science and Technology of Japan, grants from the Organization for Pharmaceutical Safety and Research, and a grant from Japan Science and Technology Cooperation.

References

[1] A.A. Avilion, S.K. Nicolis, L.H. Pevny, L. Perez, N. Vivian, R. Lovell-Badge, Multipotent cell lineages in early mouse development depend on SOX2 function, Genes Dev. 17 (2003) 126–140.
[2] M.C. Bennett, J.F. Bishop, Y. Leng, P.B. Chock, T.N. Chase, M.M. Mouradian, Degradation of alpha-synuclein by proteasome, J. Biol. Chem. 274 (1999) 33855–33858.
[3] K.K.K. Chung, Y. Zhang, K.L. Lim, Y. Tanaka, H. Huang, J. Gao, et al., Parkin ubiquitinates the α-synuclein-interacting protein, synphilin-1: implications for Lewy-body formation in Parkinson disease, Nat. Med. 7 (2001) 1144–1150.
[4] A. Ciechanover, A.L. Schwartz, The ubiquitin–proteasome pathway: the complexity and myriad functions of proteins death, Proc. Natl. Acad. Sci. U. S. A. 95 (1998) 2727–2730.
[5] I.N. Day, L.J. Hinks, R.J. Thompson, The structure of the human gene encoding protein gene product 9.5 (PGP9.5), a neuron-specific ubiquitin C-terminal hydrolase, Biochem. J. 268 (1990) 521–524.
[6] M.C. DeRijk, C. Tzourio, M.M.B. Breteler, J.F. Dartigues, L. Amaducci, S. Lopez-Pousa, et al., Prevalence of parkinsonism and Parkinson's disease in Europe: the EUROPARKINSON collaborative study, J. Neurol. Neurosurg. Psychiatry 62 (1997) 10–15.
[7] R. Dono, Fibroblast growth factors as regulators of central nervous system development and function, Am. J. Physiol., Regul. Integr. Comp. Physiol. 284 (2003) R867–R881.
[8] E. Eytan, T. Armon, H. Heller, S. Beck, A. Hershko, Ubiquitin C-terminal hydrolase activity associated with the 26S protease complex, J. Biol. Chem. 268 (1993) 4668–4674.
[9] J. Fantes, N.K. Ragge, S.A. Lynch, N.I. McGill, J.R. Collin, P.N. Howard-Peebles, C. Hayward, A.J. Vivian, K. Williamson, V. Van Heyningen, D.R. Fitz Patrick, Mutations in SOX2 cause anophthalmia, Nat. Genet. 33 (2003) 461–463.
[10] L.I. Golbe, G. Di Iorio, G. Sanges, A.M. Lazzarini, S. La Salsa, V. Bonavita, et al., Clinical genetic analysis of Parkinson's disease in the Contursi kindred, Ann. Neurol. 40 (1996) 767–775.
[11] T. Hattori, N. Ohoka, Y. Inoue, H. Hayashi, K. Onozaki, C/EBP family transcription factors are degraded by the proteasome but stabilized by forming dimmer, Oncogene 22 (2003) 1273–1280.

[12] C.E. Henderson, W. Camu, C. Mettling, A. Gouin, K. Poulsen, M. Karihaloo, J. Ruliamas, T. Evans, S.B. McMahon, M.P. Armanini, L. Berkemeier, H.S. Phillips, A. Rosenthal, Neurotrophins promote motor neuron survival and are present in embryonic limb bud, Nature 364 (1993) 266–270.
[13] N. Ichihara, J. Wu, D.H. Chui, K. Yamazaki, T. Wakabayashi, T. Kikuchi, Axonal degeneration promotes abnormal accumulation of amyloid beta-protein in ascending gracile tract of gracile axonal dystrophy (GAD) mouse, Brain Res. 695 (1995) 173–178.
[14] B.L. Kagan, R.T. Henke, R. Cabal-Manzano, G.E. Stoica, Q. Nguyen, A. Wellstein, A.T. Riegel, Complex regulation of the fibroblast growth factor-binding protein in MDA-MB-468 breast cancer cells by CCAAT/Enhancer-binding protein beta, Cancer Res. 63 (2003) 1696–1705.
[15] T. Kikuchi, M. Mukoyama, K. Yamazaki, H. Moriya, Axonal degeneration of ascending sensory neurons in gracile axonal dystrophy mutant mouse, Acta Neuropathol. 80 (1990) 145–151.
[16] Y.H. Kim, C.Y. Choi, S.-J. Lee, M.A. Conti, Y. Kim, Homeodomain-interacting protein kinases, a novel family of co-repressors for homeodomain transcription factors, J. Biol. Chem. 273 (1998) 25875–25879.
[17] T. Kitada, S. Asakawa, N. Hattori, H. Matsumine, Y. Yamamura, S. Minoshima, et al., Mutations in the parkin gene cause autosomal recessive juvenile parkinsonism, Nature (London) 392 (1998) 605–608.
[18] R. Kruger, W. Kuhn, T. Muller, D. Woitalla, M. Graeber, S. Kosel, H. Przuntek, J.T. Epplen, L. Schols, O. Riess, Ala30Pro mutation in the gene encoding alpha-synuclein in Parkinson's disease, Nat. Genet. 18 (1998) 106–108.
[19] R. Kruger, O. Eberhardt, O. Riess, J.B. Schulz, Parkinson's disease: one biochemical pathway to fit all genes? Trends Mol. Med. 8 (2002) 236–240.
[20] E. Leroy, R. Boyer, G. Auburger, B. Leube, G. Ulm, E. Mezey, G. Brownstein, M.J. Brownstein, S. Jonnalagada, T. Chernova, et al., The ubiquitin pathway in Parkinson's disease, Nature 395 (1998) 451–452.
[21] A.P. Lieberman, G. Harmison, A.D. Strand, J.M. Olson, K.H. Fischbeck, Altered transcriptional regulation in cells expressing the expanded polyglutamine androgen receptor, Hum. Mol. Genet. 11 (2002) 1967–1976.
[22] G. Liu, A.E. Loraine, R. Shigeta, M. Cline, J. Cheng, V. Valmeekam, S. Sun, D. Kulp, M.A. Siani-Rose, NetAffx: affymetrix probesets and annotations, Nucleic Acids Res. 31 (2003) 82–86.
[23] Y. Liu, L. Fallon, H.A. Lashuel, Z. Liu , P.T. Lansbury Jr., The UCH-L1 gene encodes two opposing enzymatic activities that affect alpha-synuclein degradation and Parkinson's disease susceptibility, Cell 111 (2002) 209–218.
[24] A.M. Lohof, Y. Ip, M. Poo, Potentiation of developing neuromuscular synapses by the neurotrophins NT-3 and BDNF, Nature 363 (1993) 350–353.
[25] J. Lowe, H. McDermott, M. Landon, R.J. Mayer, K.D. Wilkinson, Ubiquitin carboxyl-terminal hydrolase (PGP 9.5) is selectively present in ubiquitinated inclusion bodies characteristic of human neurodegenerative diseases, J. Pathol. 161 (1990) 153–160.
[26] C.B. Lücking, A. Dürr, V. Bonifati, J. Vaugham, G. De Michele, T. Gasser, et al., Association between early-onset Parkinson's disease and mutations in the parkin gene, N. Engl. J. Med. 342 (2000) 1560–1567.
[27] D.M. Maraganore, M.J. Farrer, J.A. Hardy, S.J. Lincoln, S.K. McDonnell, W.A. Rocca, Case-control study of the ubiquitin carboxy-terminal hydrolase L1 gene in Parkinson's disease, Neurology 53 (1999) 1858–1860.
[28] F.P. Marx, C. Holzmann, K.M. Strauss, L. Li, O. Eberhard, M. Cookson, et al., Identification and functional characterization of a novel R621C mutation in the synphilin-1 gene in Parkinson's disease, Hum. Mol. Genet. 12 (2003) 1223–1231.
[29] K. Matsui, S. Furukawa, J.-G. Suh, K. Wada, Developmental changes of nerve growth factor levels in the gracile axonal dystrophy mouse, Neurosci. Lett. 177 (1994) 116–118.
[30] K.S. McNaught, L.M. Bjorklund, R. Belizaire, O. Isacson, P. Jenner, C.W. Olanow, Proteasome inhibition causes nigral degeneration with inclusion bodies in rats, NeuroReport 13 (2002) 1437–14411.
[31] D.J. Nicholl, J.R. Vaughan, N.L. Khan, S.L. Ho, D.E.W. Aldous, S. Lincoln, et al., Two large British kindreds with familial Parkinson's disease: a clinico-pathological and genetic study, Brain 125 (2002) 44–57.
[32] K. Nishikawa, H. Li, R. Kawamura, H. Osaka, Y.L. Wang, Y. Hara, et al., Alterations of structure and hydrolase activity of parkinsonism-associated human ubiquitin carboxyl-terminal hydrolase L1 variants, Biochem. Biophys. Res. Commun. 304 (2003) 176–183.
[33] H. Osaka, Y.L. Wang, K. Takada, S. Takizawa, R. Setsuie, H. Li, Y. Sato, et al., Ubiquitin carboxy-terminal hydrolase L1 binds to and stabilizes monoubiquitin in neuron, Hum. Mol. Genet. 12 (2003) 1945–1958.
[34] E. Ozkaynak, D. Finley, M.J. Solomon, A. Varshavsky, The yeast ubiquitin genes: a family of natural gene fusions, EMBO J. 6 (1987) 1429–1439.
[35] P. Piccini, D.J. Burn, R. Ceravolo, D. Maraganore, D.J. Brooks, The role of inheritance in sporadic Parkinson's disease: evidence from a longitudinal study of dopaminergic function in twins, Ann. Neurol. 45 (1999) 577–582.
[36] M.H. Polymeropoulos, C. Lavedan, E. Leroy, S.E. Ide, A. Dehejia, A. Dutra, B. Pike, H. Root, J. Rubenstein, R. Boyer, E.S. Stenroos, S. Chandrasekharappa, A. Athanassiadou, T. Papapetropoulos, W.G. Johnson, A.M. Lazzarini, R.C. Duvoisin, G. Di Iorio, L.I. Golbe, R.L. Nussbaum, Mutation in the alpha-synuclein gene identified in families with Parkinson's disease, Science 276 (1997) 2045–2047.
[37] K. Saigoh, Y.L. Wang, J.G. Suh, T. Yamanishi, Y. Sakai, H. Kiyosawa, T. Harada, N. Ichihara, S. Wakana, T. Kikuchi, K. Wada, Intragenic deletion in the gene encoding ubiquitin carboxy-terminal hydrolase in gad mice, Nat. Genet. 23 (1999) 47–51.
[38] H. Shimura, N. Hattori, S.-I. Kubo, Y. Mizuno, S. Asakawa, S. Minoshima, et al., Familial Parkinson disease gene product, parkin, is a ubiquitin-protein ligase, Nat. Genet. 25 (2000) 302–305.
[39] A. Sturn, J. Quackenbush, Z. Trajanoski, Genesis: cluster analysis of microarray data, Bioinformatics 18 (2002) 207–208.
[40] G.K. Tofaris, R. Layfield, M.G. Spillantini, Alpha-synuclein metabolism and aggregation is linked to ubiquitin-independent degradation by the proteasome, FEBS Lett. 509 (2001) 22–26.
[41] K.D. Wilkinson, K.M. Lee, S. Deshpande, P. Duerksen-Hughes, J.M. Boss, J. Pohl, The neuron-specific protein PGP 9.5 is a ubiquitin carboxyl-terminal hydrolase, Science 246 (1989) 670–673.
[42] P. Winteimeyer, R. Krüger, W. Kuhn, T. Müller, D. Woitalla, D. Berg, et al., Mutation analysis and association studies of the UCHL1 gene in German Parkinson's disease patients, NeuroReport 11 (2000) 2079–2082.
[43] Z.K. Wszolek, B. Pfeiffer, J.R. Fulgham, J.E. Parisi, B.M. Thompson, R.J. Uitti, et al., Western Nebraska family (family-D) with autosomal dominant parkinsonism, Neurology 45 (1995) 502–505.
[44] K. Yamazaki, H. Moriya, N. Ichihara, H. Mitsushio, S. Inagaki, T. Kikuchi, Substance P-immunoreactive astrocytes in gracile sensory nervous tract of spinal cord in gracile axonal dystrophy mutant mouse, Mol. Chem. Neuropathol. 20 (1993) 1–20.

Journal of Neurochemistry, 2004, **88**, 1540–1546 doi:10.1046/j.1471-4159.2003.02288.x

Proteomic analysis of brain proteins in the gracile axonal dystrophy (*gad*) mouse, a syndrome that emanates from dysfunctional ubiquitin carboxyl-terminal hydrolase L-1, reveals oxidation of key proteins

Alessandra Castegna,* Visith Thongboonkerd,** Jon Klein,** Bert C. Lynn,*,†,‡ Yu-Lai Wang,§ Hitoshi Osaka,§,¶ Keiji Wada,§ and D. Allan Butterfield*,‡

**Department of Chemistry and Center of Membrane Sciences, †Core Proteomics Laboratory and ‡Sanders-Brown Center on Aging, University of Kentucky, Lexington, Kentucky 40506 USA*

§Department of Degenerative Neurological Diseases, National Institute of Neuroscience, Tokyo, Japan

¶PRESTO, Japan Science and Technology Corporation, Saitama, Japan

***Kidney Disease Program and Proteomics Core Laboratory, University of Louisville, Louisville, Kentucky, USA*

Abstract

Ubiquitin carboxyl-terminal hydrolase L-1 (UCH L-1) is a crucial enzyme for proteasomal protein degradation that generates free monomeric ubiquitin. Our previous proteomic study identified UCH L-1 as one specific target of protein oxidation in Alzheimer's disease (AD) brain, establishing a link between the effect of oxidative stress on protein and the proteasomal dysfunction in AD. However, it is unclear how protein oxidation affects function, owing to the different responses of proteins to oxidation. Analysis of systems in which the oxidized protein displays lowered or null activity might be an excellent model for investigating the effect of the protein of interest in cellular metabolism and evaluating how the cell responds to the stress caused by oxidation of a specific protein. The gracile axonal dystrophy (*gad*) mouse is an autosomal recessive spontaneous mutant with a deletion on chromosome 5 within the gene encoding UCH L-1. The mouse displays axonal degeneration of the gracile tract. The aim of this proteomic study on *gad* mouse brain, with dysfunctional UCH L-1, was to determine differences in brain protein oxidation levels between control and *gad* samples. The results showed increased protein oxidation in thioredoxin peroxidase (peroxiredoxin), phosphoglycerate mutase, Rab GDP dissociation inhibitor α/ATP synthase and neurofilament-L in the *gad* mouse brain. These findings are discussed with reference to the effect of specific protein oxidation on potential mechanisms of neurodegeneration that pertain to the *gad* mouse.

Keywords: Alzheimer's disease, amyotrophic lateral sclerosis, brain protein oxidation, proteasome, proteomics, ubiquitin carboxyl terminal hydrolase L-1.

J. Neurochem. (2004) **88**, 1540–1546.

The gracile axonal dystrophy (*gad*) mouse is an autosomal recessive spontaneous mutant that was identified in 1984 (Yamazaki *et al.* 1988). Pathologically, the *gad* mouse displays axonal degeneration of the gracile tract, which consists of thoracic, lumbar and sacral dorsal root ganglion axons. This axonal deterioration results in progressive sensory ataxia, and eventually spreads to the motor neurons and other centers in the CNS, causing paralysis and death after 150 days of age (Yamazaki *et al.* 1988). Accumulation of ubiquitin and amyloid-β protein deposits is also present along the sensory and motor nervous system (Wu *et al.* 1996).

Received October 14, 2003; revised manuscript received November 18, 2003; accepted November 20, 2003.

Address correspondence and reprint requests to Professor D. Allan Butterfield, Department of Chemistry and Center of Membrane Sciences, University of Kentucky, Lexington, KY 40506-0055, USA.
E-mail: dabcns@uky.edu

Abbreviations used: AD, Alzheimer's disease; DNP, dinitrophenyl hydrazone; DNPH, 2,4-dinitrophenylhydrazine; 2D PAGE, two-dimensional polyacrylamide gel electrophoresis; IPG, immobilized pH gradient; MS/MS, tandem mass spectrometry; UCH L-1, ubiquitin carboxyl-terminal hydrolase L-1.

The *gad* mutation has been identified as a deletion on chromosome 5 within the gene encoding ubiquitin carboxyl-terminal hydrolase L-1 (UCH-L1). The deletion lacks a segment of DNA corresponding to 42 amino acids containing the catalytic site of this protein (Saigoh *et al.* 1999). The role of UCH-L1 renders this mouse a suitable model for investigating neurodegenerative disorders, in which altered function of the ubiquitin system is present.

UCH L-1 is a crucial enzyme for maintaining protein degradation by the proteasome, by generating free monomeric ubiquitin (Osaka *et al.* 2003). Proteasomal dysfunction occurs in neurodegenerative disorders (Chung *et al.* 2001; Davies 2001; Ding and Keller 2001; Halliwell 2002). In Parkinson's disease there is genetic evidence for a contribution of UCH L-1 (Liu *et al.* 2002; Nishikawa *et al.* 2003; Jenner 2003). Our previous proteomic study (Castegna *et al.* 2002a) identified UCH L-1 as one specific target of protein oxidation in Alzheimer's disease (AD) brain, establishing a link between the effect of oxidative stress of brain proteins (Butterfield and Lauderback 2002; Butterfield *et al.* 2001; 2002) and the reported proteasomal dysfunction in AD. However, it is unclear how oxidation affects protein function, owing to the different responses of proteins to oxidation. Analysis of systems in which the oxidized protein displays lowered or null activity might represent an excellent model for investigating the effect of the protein of interest in cellular metabolism and evaluating how the cell responds to the stress caused by its oxidation.

Because of the lack of activity of UCHL-1 in *gad* mouse brain, this animal model was chosen to investigate the effect of dysfunctional UCH-L1 in brain in relation to specifically oxidized proteins. Proteomics appeared to be the most efficient way of performing this study because this method allows screening of both the expression and oxidation of hundreds of proteins at once.

Experimental procedures

Brain samples

Six wild-type and six *gad* mouse brain cortical samples (300 mg) were sonicated for 30 s in 500 μL two-dimensional polyacrylamide gel electrophoresis (2D PAGE) sample buffer (8 M urea, 2 M thiourea, 20 mM dithiothreitol, 0.2% (v/v) Biolytes 3–10, 2% CHAPS and bromophenol blue). Following centrifugation at 14000 *g* for 10 min, the supernatant was collected and the protein concentration was determined by using the RC DC assay (Bio-Rad, Hercules, CA, USA) as described previously (Castegna *et al.* 2002a,b, 2003).

2D PAGE and western blotting

2D PAGE was performed in a Bio-Rad system using 110-mm pH 3–10 immobilized pH gradient (IPG) strips and Criterion 8–16% gels (Bio-Rad). For the first dimension, 300 μg protein was applied to a rehydrated IPG strip, and isoelectric focusing was carried out at 20°C. Before the second-dimension separation, the gel strips were equilibrated for 10 min in 37.5 mM Tris-HCl (pH 8.8) containing 6 M urea, 2% (w/v) sodium dodecyl sulfate, 20% (v/v) glycerol and 0.5% dithiothreitol, and then re-equilibrated for 10 min in the same buffer except that dithiothreitol was replaced with 4.5% iodoacetamide. For detection of protein carbonyls, an index of protein oxidation (Butterfield and Stadtman 1997), Western blots (oxyblots) were obtained. The protein hydrazone was formed by incubating IPG strips with 10 mM 2,4-dinitrophenylhydrazine (DNPH)/1 M HCl for 10 min and 2 M Tris base/30% glycerol for 15 min. A detailed description of the chemistry involved in protein carbonyl formation and analysis has been published (Butterfield and Stadtman 1997). Basically, in the present study protein carbonyls were detected immunochemically by an antibody to the hydrazone formed between protein carbonyls and DNPH, followed by an alkaline phosphate-linked secondary antibody (Castegna *et al.* 2002a,b). The IPG strips were rehydrated as described above and placed on Criterion gels (Bio-Rad). After unstained molecular weight protein standards had been applied, electrophoresis was started. Isoelectric focusing was performed as follows: 300 V for 1 h, then linear gradient to 8000 V for 5 h and finally 20 000 V/h. Second-dimension gels were run at 200 V for 65 min (Butterfield and Castegna 2003). Immunoblotting analysis was performed as described in Castegna *et al.* (2002a).

Sample preparation for matrix-assisted laser desorption ionization-time of flight (MALDI-TOF) mass spectrometry

All mass spectra reported in this study were acquired by the University of Kentucky Mass Spectrometry Facility with an HP 1100 HPLC system modified with a custom splitter to deliver 4 μL/min to a custom C18 capillary column [300 μm (internal diameter) × 15 cm, packed in-house with Macrophere 300 5-μm C18 ; Alltech Associates, Deerfield, IL, USA]. Gradient separations consisted of 2 min isocratic at 95% water : 5% acetonitrile (both phases contain 0.1% formic acid) to begin with; the organic phase was increased to 20% acetonitrile over 8 min, then increased to 90% acetonitrile over 25 min, held at 90% acetonitrile for 8 min, then increased to 95% for 2 min, and finally returned to initial conditions for 10 min (total acquisition time 45 min with a 10-min recycle time). Tandem mass spectrometry (MS/MS) spectra were acquired on a Finnigan LCQ 'Classic' quadrupole ion trap mass spectrometer (Finnigan, Co., San Jose, CA, USA) in a data-dependent manner. Three scans were averaged to generate the data-dependent full scan spectrum. The most intense ion was subjected to tandem mass spectrometry, and five scans were averaged to produce the MS/MS spectrum. Masses subjected to the MS/MS scan were placed on an exclusion list for 2 min.

Tandem spectra used for protein identification from tryptic fragments were searched against the National Center for Biotechnology Information (NCBI) protein databases using a local MASCOT search engine server. Resulting MS/MS spectra assumed the peptides to be mono-isotopic, oxidized at methionine residues and carbamidomethylated at cysteine residues (Castegna *et al.* 2002a,b, 2003). However, a 0.8-Da MS/MS mass tolerance was used for searching. Only the MS/MS data provided identification of proteins, and a typical mass spectrum is represented in Fig. 1.

Probability-based MOWSE scores were estimated by comparison of search results against estimated random match population and were reported as $-10*\mathrm{LOG10}(p)$, where p is the absolute probab-

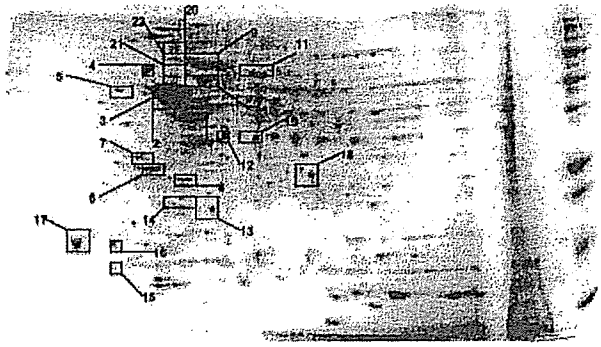

#	Protein
1	β-actin
2	Enolase
3	Tubulin
4	Neurofilament
5	Neurofilament
6	Tyrosine-3-monoyxygenase
7	tyrosine 3/tryptophan 5 -monooxygenase activation protein
8	Rho GDP-dissociation inhibitor I
9	Heat shock cognate 71 kDa protein
10	neurofilament protein NF-66
11	dihydropyrimidinase related protein-2
12	lactate dehydrogenase 2
13	RIKEN cDNA
14	thioredoxin peroxidase
15	hippocampal cholinergic neurostimulating peptide precursor
16	protein
17	β-synuclein
18	Calmodulin
19	phosphoglycerate mutase
20	malate dehydrogenase
21	Heat shock protein 86
22	dnaK-type molecular chaperone grp78 precursor or 78 kDa glucose-regulated protein precursor (GRP 78) Rab GDP dissociation inhibitor alpha & ATP synthase

Fig. 1 Example of liquid chromatography–MS/MS spectrum. In this case the spectrum is *m/z* 968 from gi/25742763 70-kDa heat-shock protein.

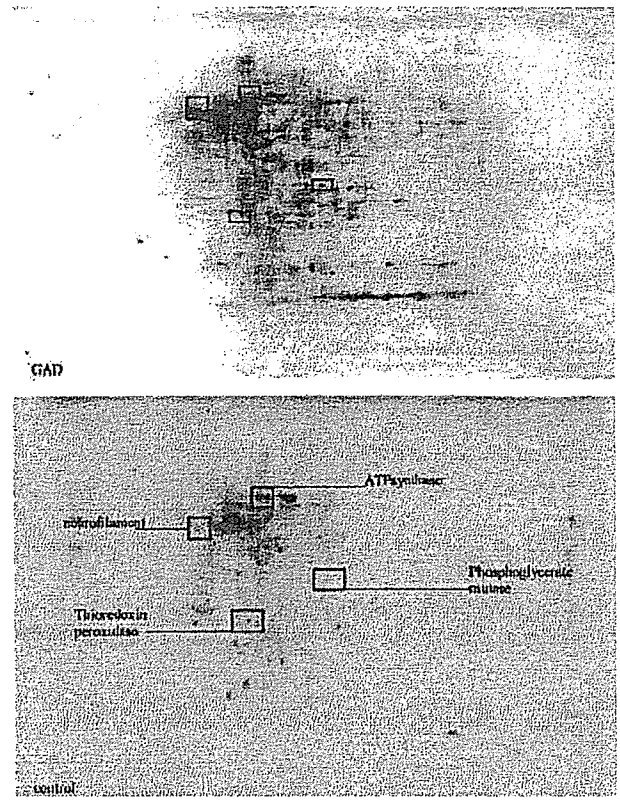

Fig. 2 D gel map of *gad* mouse brain. The proteins corresponding to the 22 spots identified by mass spectrometry are listed. As with most 2D gels, the pH increases from left to right on the abscissa, and molecular mass decreases from top to bottom on the ordinate.

ility. All protein identifications were in the expected size range based on position in the gel.

Statistical analysis

Statistical comparison of carbonyl levels of proteins with anti-dinitrophenyl hydrazone (anti-DNP)-positive spots on 2D oxyblots from *gad* and wild-type, aged-matched control brain samples was by ANOVA. $p < 0.05$ was considered significantly different.

Results

DNPH-positive proteins on the blot were located in the gel map and excised for mass spectrometric analysis as described above. Twenty-two proteins were identified (Fig. 2). Proteins containing reactive carbonyl groups in *gad* and control brain samples were identified by 2D oxyblot analysis (Fig. 3). Comparison of 2D oxyblots with images of Coomassie blue-stained 2D gels from the same samples revealed that many, but not all, individual protein spots in the inferior parietal lobule brain extracts exhibit anti-protein carbonyl immunoreactivity. 2D oxyblots and the subsequent 2D gel images were matched and the anti-DNP immunoreactivity of individual proteins separated by 2D PAGE was normalized to their protein content, obtained by measuring the intensity of colloidal Coomassie blue staining. This procedure allowed comparison of oxidation levels of brain proteins in *gad* and control subjects (Castegna *et al.* 2002a,b; Butterfield and Castegna 2003; Butterfield *et al.* 2003).

Only four proteins exhibited a significant increase in protein carbonyls in *gad* compared with control samples (Table 1). Three of these proteins were identified as phosphoglycerate mutase (1025 ± 187% of control), thioredoxin peroxidase (708 ± 123% of control) and neurofilament L (NF-L) (853 ± 13% of control). ATP synthase was identified together with Rab GDP dissociation inhibitor α; these two proteins have the same isoelectric point (pI) and molecular mass and it was impossible to separate them by 2D PAGE. The oxidation level for this mixture was 154 ± 43% of the wild-type spot. Table 2 presents the unique protein identifier (GI accession number), number of peptides identified, sequences determined, percentage sequence coverage, the probability-based MOWSE score and the *p* value for each oxidized protein identified. Note that the latter is exceedingly small, indicating that the identity established for each protein is correct.

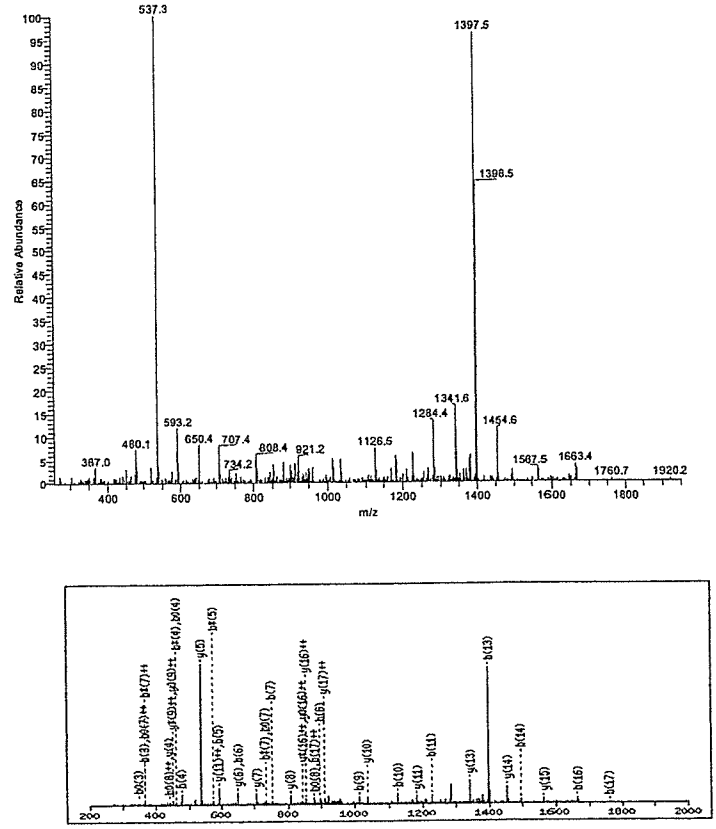

Fig. 3 Oxyblot maps for *gad* (top) and wild-type (bottom) mouse brain proteins, with labeled proteins significantly more oxidized in the *gad* mouse brain samples. The axes are the same as those in Fig. 1.

Discussion

The presence of non-functional UCH L1 in the *gad* mouse results in severe motor neuronal impairment. The results presented here give insight for the first time into the mechanism of neuronal degeneration in the *gad* mouse. Oxidative stress is responsible for NF-L disassembly, which in turn impairs axonal transport, causes demyelination and eventually leads to neuronal atrophy and death.

Table 1 Relative percentage change in specific carbonyl levels in proteomics-identified proteins in *gad* mouse brain compared with wild-type mouse control brain

Identified protein	Specific oxidation (% of control)	p^*
Phosphoglycerate mutase	1025 ± 187	0.05
Thioredoxin peroxidase	708 ± 123	< 0.05
Rab/ATPase (?)	154 ± 43	< 0.04
NF-L	853 ± 13	< 0.04

For each protein, individual anti-DNP immunostain/protein values (obtained from each of six *gad* and six control brains) were averaged and expressed as percentage of control ± SEM. *ANOVA.

Neurofilaments are axonal proteins that participate in the neuronal cytoskeletal structure and play an important role in the process of myelination. NF-L is a target of intensive study in motor neuron disease, in which abnormalities of its assembly, secondary structure and post-translational modifications have been detected (Crow *et al.* 1997; Beckman 1996; Chou *et al.* 1998; Cookson and Shaw 1999; Gelinas *et al.* 2000).

The abnormal accumulation of NF-L in degenerated motor neurons, which is the main pathological feature of amyotrophic lateral sclerosis (ALS), has initiated studies of the relationship between superoxide dismutase 1 mutation, which occurs in familial cases of ALS, and neurofilament accumulation. Superoxide dismutase-initiated nitration of mouse disassembled NF-L showed increases in 3-nitrotyrosine (Crow *et al.* 1997), consistent with the finding that tyrosine is often responsible for stabilization of neurofilament subunits, a stabilization fostered by hydrophobic interactions (Heins *et al.* 1993). Additionally, transgenic mice expressing a point mutation of NF-L exhibit motor impairment (Cote *et al.* 1993).

The hypothesis that neurofilaments might be a target of protein modification in motor neuron diseases in supported by extensive evidence (Beckman 1996; Chou *et al.* 1998; Cookson and Shaw 1999). Other than being targets of protein

Table 2 Proteomics characteristics of oxidatively modified proteins identified in *gad* mouse brain

Identified protein	GI accession no.	No. of peptides	Sequence	Sequence coverage (%)	MOWSE score	*p*
Phosphoglycerate mutase	gil8248819	5	LVLIR KAMEAVAAQGK + Oxidation(M) VLIAAHGNSLR NLKPIKPMQFLGDEETVR + Oxidation(M) HLEGLSEEAIMELNLPTGIPIVYELDK + Oxidation(M)	28	228	1.60×10^{-23}
Thioredoxin peroxidase (peroxiredoxin 2)	gil2499469	9	GVLR EYFSK SVDEALR GLFIIDAK NDEGIAYR SLSQNYGVLK SAPDFTATAVVDGAFK EGGLGPLNIPLLADVTK KEGGLGPLNIPLLADVTK	38	330	1.00×10^{-33}
Rab GDP dissociation inhibitor α	gil21903424	8	VVGVK LYSESLAR VVEGSFVYK FLMANGQLVK + Oxidation(M) KQNDVFGEADQ FQMLEGPPESMGR + 2Oxidation(M) NPYYGGESSSITPLEELYK YIAIASTTVETAEPEKEVEPALELLEPIDQK	23	388	1.60×10^{-39}
NF-L	gil20876600	20	DLR YVETPR LENELR FASFIER LLEGEETR KGADEAALAR ALYEQEIR YEEEVLSR LAAEDATNEK FTVLTESAAK AQLQDLNDR EYQDLLNVK VHELEQQNK MALDIEIAAYR + Oxidation(M) NMQNAEEWFK + Oxidation(M) IDSLMDEIAFLK + Oxidation(M) QNADISAMQDTINK + Oxidation(M) RIDSLMDEIAFLK + Oxidation(M) SAYSGLQSSSYLMSAR + Oxidation(M) SFPAYYTSHVQEEQTEVEETIEATK	35	864	3.90×10^{-87}

Oxidation (M); Oxidation of methionine.

nitration in ALS, neurofilament aggregates also bear advanced glycation endproducts in ALS conglomerates, indicating the susceptibility of neurofilament-L to oxidative insult.

The present finding of oxidized NF-L in *gad* mouse brain, a model for neuron motor disease, confirms previous data that provided evidence for the oxidation-related involvement of NF-L in motor neuron degeneration and established a common pattern for degeneration. If the results shown here for cortical tissue can be extended to spinal cord and motor neurons, the findings may be relevant to molecular mechanisms of neurodegeneration in ALS. Oxidation of NF-L implies modification of hydrophobic interactions that are responsible for the association of the different subunits. In fact, it has been demonstrated that the structure of neurofilament proteins is modified from α-helix to β-sheet

and random coil following free radical damage (Gelinas *et al.* 2000), directly relating oxidative damage of neurofilaments to the axonal degeneration in motor neurons. The consequences of neurofilament disassembly are deleterious to neuronal survival: the axonal antegrade and retrograde transport, which is essential for organelles, especially mitochondria which do not self-sufficiently synthesize most of the proteins necessary for their function, would be compromised.

Reduction of the fixed ubiquitin pool and decreased proteasomal function might lead to accumulation of oxidized proteins, which, in turn, might activate microglia and trigger an inflammatory response with production of free radicals. Such events, which might lead to neurodegeneration, might be exacerbated by the oxidation of thioredoxin peroxidase, which was also a target of oxidation in this *gad* mouse model of neurodegeneration. Thioredoxin peroxidases or peroxiredoxins are small redox proteins that act as antioxidants and catalyze the elimination of hydroperoxides through the reducing system thioredoxin/thioredoxin reductase. This enzyme is considered a strong defense against oxidative stress. Based on the loss of activity of other oxidatively modified brain proteins (Hensley *et al.* 1995; Butterfield *et al.* 1997), the finding of the present study that thioredoxin peroxidase is a target of protein oxidation in *gad* mouse brain implies harmful consequences for neurons in this UCH L-1-altered mouse, owing to a dramatic decrease in cellular antioxidant capability. Peroxiredoxin I/thioredoxin peroxidase 2 is up-regulated in ALS (Allen *et al.* 2003). Moreover, in oxidative stress induced by Fe^{2+} (Drake *et al.* 2002) or H_2O_2 (Mitsumoto *et al.* 2001) variant forms of peroxiredoxins have been identified. These investigations by others, coupled with the present finding that peroxiredoxin is oxidized in the *gad* mouse, are consistent with the existence of common downstream events in oxidative stress-induced neurodegeneration.

An oxidative stress-based mechanism of peroxiredoxin enzyme inactivation can be speculated: the enzyme bears two cysteine residues that are crucial for the antioxidant activity of thioredoxin peroxidase. Products of free radical-induced lipid peroxidation, such as 4-hydroxy-2-nonenal, can introduce carbonyls to proteins by covalent Michael addition to -SH groups of protein side chains (Butterfield and Stadtman 1997; Lauderback *et al.* 2001). Thus, it is conceivable that these cysteine proteins in peroxiredoxin are susceptible to attack by the excess 4-hydroxy-2-nonenal in neurodegenerative disorders associated with oxidative stress, including AD. Michael addition of 4-hydroxy-2-nonenal to brain proteins changes their structure and activity (Esterbauer *et al.* 1991; Subramaniam *et al.* 1997; Lauderback *et al.* 2001).

Phosphoglycerate mutase is the glycolytic enzyme responsible for the interconversion of 3-phosphoglycerate to 2-phosphoglycerate. Glycolytic enzymes and creatine kinase BB are oxidatively modified in AD brain (Castegna *et al.* 2002a, 2002b, 2003; Butterfield and Castegna 2003; Butterfield *et al.* 2003), and this oxidation might contribute to the reduced glucose metabolism observed in AD brain (Messier and Gagnon 1996), especially in the temporoparietal and frontal areas (Mielke *et al.* 1996). Although there is no evidence of involvement of energy metabolism depletion in the *gad* brain, the present finding that phosphoglycerate mutase was significantly more oxidized in *gad* brain than in control brain suggests a possible lower energy metabolism that might exacerbate the consequences of a lack of ATP necessary to carry out normal cellular function. Future studies should address this possibility.

Rab GDP dissociation inhibitor α and ATP synthase were detected as a single spot on the *gad* brain map, and the spot corresponding to these proteins showed increased carbonyl immunoreactivity. It is not possible at the present time to distinguish the extent of oxidation for the two proteins, the pI and molecular mass of which are practically identical. This result illustrates a limitation of 2D PAGE in separating proteins of similar size and charge distribution. Additional studies are required, perhaps using different isoelectric focusing strips with wider pH gradients, to separate the mixture into two detectable spots.

As seen in the present study, oxidative stress may be a source of protein damage by a vicious cycle, in which targets of oxidation may lead to further damage, as in the *gad* mouse. Further study of these connections is warranted. The present study demonstrates how the powerful tools of proteomics can provide insights into potential mechanisms of neurodegenerative disease. Continued use of proteomics analysis for the brain proteome in oxidative stress-related neurodegenerative disorders, and animal and culture models thereof, is in progress.

Acknowledgements

This work was supported in part by grants from the National Institutes of Health to DAB (AG-05119; AG-10836) and JK (R01 HL66358-01), and grants from the Ministry of Health, Labour and Welfare of Japan to KW and the Organization for Pharmaceutical Safety and Research of Japan to KW (MF-3).

References

Allen S., Heath P. R., Kirby J., Wharton S. B., Cookson M. R., Menzies F. M., Banks R. E. and Shaw P. J. (2003) Analysis of the cytosolic proteome in a cell culture model of familial amyotrophic lateral sclerosis reveals alterations to the proteasome, antioxidant defenses, and nitric oxide synthetic pathways. *J. Biol. Chem.* **278**, 6371–6383.

Beckman J. S. (1996) Oxidative damage and tyrosine nitration from peroxynitrite. *Chem. Res. Toxicol.* **9**, 836–844.

Butterfield D. A. and Lauderback C. M. (2002) Lipid peroxidation and protein oxidation in Alzheimer's disease brain: potential causes and consequences involving amyloid β-peptide-associated free radical oxidative stress. *Free Rad. Biol. Med.* **32**, 1050–1060.